Modeling of Opto-Electronics in Complex Photonic Integrated Circuits

C. Arellano[1a], S. Mingaleev[b], I. Koltchanov[a], A. Richter[a]
[a]VPIphotonics GmbH, Carnotstr. 6, 10587 Berlin, Germany;
[b]VPI Development Center, Chapaeva str. 5, 220034 Minsk, Belarus.

ABSTRACT

This work addresses a versatile modeling of complex photonic integrated circuits (PICs) including optical and electrical sub-elements. We introduce a new family of electrical elements, together with a novel electronic-photonic co-design, that complements current capabilities of photonic circuit simulators. This is illustrated with the modeling of complex electric circuits contained in photonic devices. Simulations of the interaction between electrical and optical parts allow the analysis of unwanted effects such as reflections due to impedance mismatching, as well as the optimization of the PIC as a whole.

We illustrate the functionalities of our approach through application examples. As a use case, we present a model of the electrical driver for a monolithically-integrated InP transmitter developed in frame of the European research project MIRTHE and the analysis of the driver and the EA-Modulator interplay.

1. INTRODUCTION

Circuit level modeling of photonic integrated circuits (PICs) encompassing electronic-photonic co-design is one of the main requirements for enabling rapid functional design of CMOS-silicon devices as well as InP-based structures. The circuit modeling approach employed for this work covers the design of PICs that comprise elements of versatile nature as active semiconductor-based structures, passive waveguide elements and electric elements.

In previous works we have addressed the modeling of fully passive PICs, based on the description of PIC elements in terms of frequency-dependent scattering-matrices [1]. Lately, we presented a new method for efficient modeling of hybrid large-scale PICs containing active sections as well that aids inefficiencies of pure time-domain simulations [2]. We named it time-and-frequency domain modeling (TFDM).

In this contribution we present another functionality extension of *VPIcomponentMaker Photonic Circuits*, our modeling environment that allows the design of complex PICs comprising optical and linear electrical sub-elements in a single simulation setup. We connect electrical elements with each other via bidirectional ports representing forward and backward propagating electrical waves. The calculation of linear electric circuits (ECs) is then natively performed using an S-matrix approach. For this, we extended our previously developed S-matrix modeling approach for passive clusters in PICs to support the modeling of linear ECs for both, low- and high-frequency conditions.

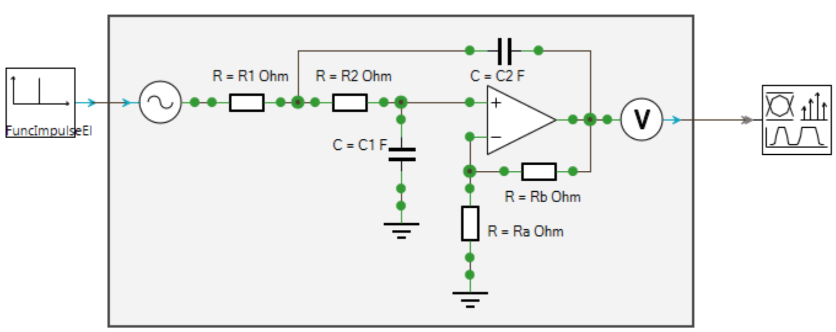

Fig. 1: Exemplary schematic of an electric circuit (Sallen-Key filter) in VPIcomponentMaker Photonic Circuits

[1] Cristina.Arellano@VPIphotonics.com, +49 30 39805830

Physics and Simulation of Optoelectronic Devices XXII, edited by Bernd Witzigmann, Marek Osinski,
Fritz Henneberger, Yasuhiko Arakawa, Proc. of SPIE Vol. 8980, 89801P · © 2014 SPIE
CCC code: 0277-786X/14/$18 · doi: 10.1117/12.2036364

2. SIMULATION OF LINEAR ELECTRIC CIRCUITS

2.1 Electrical Element Models

We have developed family of fundamental electrical elements (EEs) which allows the simulation of transmission and reflection characteristics of linear electric circuits. The collection of EEs built-in modules comprises resistors, capacitors, inductors, as well as mutual inductors, as well as independent and dependent voltage and current sources (fig. 2). The combination of fundamental EEs with the advanced cosimulation capabilities and hierarchical design approach allows efficient modeling of arbitrary types of ECs as distributed RC lines, toggle switches, ideal operational amplifiers, ideal gyrators, or any other linear electrical elements.

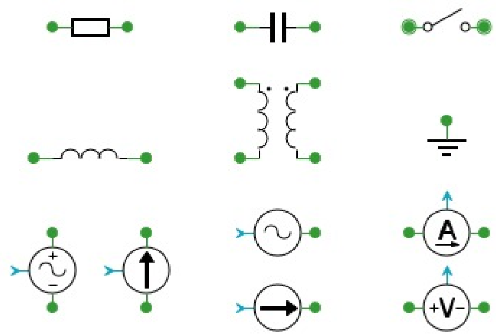

Fig. 2: Library of electrical elements for modeling linear electric circuits

We model ECs by considering them as networks of interconnected electrical devices, where each electrical device is considered as a black-box with one or several ports. Individual electrical elements are connected with each other via bidirectional ports representing forward and backward propagating electrical waves (fig. 3).

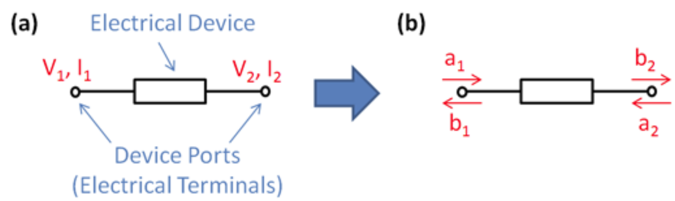

Fig. 3: Schematic view of electrical device descriptions: (a) in terms of terminals voltage and current; (b) in terms of incoming and outgoing electrical waves.

The Modified Nodal Analysis (MNA) method [3] is perhaps one of the most efficient formulations of circuit equations. This method is based on the use of admittance matrices (relating port voltages to port currents) to describe individual electrical devices, and is currently employed in most of the modern SPICE-like electronic circuits simulators [4]. Importantly, it results in a number of circuit equations which only slightly exceeds the number of electrical nodes. However, the MNA method, as well as any alternative formulation of circuit equations in terms of node voltages and/or branch currents, becomes computationally inefficient and even error-prone when it is applied to the analysis of high-frequency electronic circuits. Moreover, attempts to extend the MNA method for modeling optoelectronic circuits with even the simplest photonic devices, is a challenging task [5]. Because of this, an alternative S-matrix approach has been developed [6] and is actively used during the last decades for modeling microwave circuits. More recently, this approach has also been successfully extended for modeling photonic integrated circuits.

The S-matrix approach presented in [1] has been further developed to model linear electric circuits (both low- and high-frequency). Although this approach is computationally less efficient than the MNA method for modeling purely electronic low-frequency circuits, it is much more suitable for modeling high-frequency electronic and hybrid opto-electronic circuits.

Within the S-matrix approach, electrical terminals are described by the amplitudes a_N and b_N of incoming and outgoing electrical waves, correspondingly:

$$a_N(f) = \frac{1}{2}\left(\frac{V_N(f)}{\sqrt{R_0}} + I_N(f)\sqrt{R_0}\right) \qquad b_N(f) = \frac{1}{2}\left(\frac{V_N(f)}{\sqrt{R_0}} - I_N(f)\sqrt{R_0}\right)$$

In our model we assume that R_0 is identical for all the terminals, and is equal to 1 Ohm. This allows us to omit R_0 from all expressions, and rewrite the equations below in a more compact form:

$$a_N(f) = \frac{V_N(f)+I_N(f)}{2} \qquad b_N(f) = \frac{V_N(f)-I_N(f)}{2}$$

Each linear electrical device with N electrical terminals can be completely described, in terms of electrical traveling waves, by an NxN scattering matrix that consists of complex-valued frequency-dependent transfer functions.

$$\hat{S}(f) = \begin{pmatrix} T_{11}(f) & \cdots & T_{1N}(f) \\ \vdots & T_{mn}(f) & \vdots \\ T_{N1}(f) & \cdots & T_{NN}(f) \end{pmatrix}$$

Each transfer function $T_{mn}(f)$ relates complex amplitude $a_N(f)$ of a signal traveling towards the device port N with the complex amplitude $b_M(f)$ of a signal traveling away from the device port M:

$$\begin{pmatrix} b_1(f) \\ \cdots \\ b_N(f) \end{pmatrix} = \hat{S}(f) \begin{pmatrix} a_1(f) \\ \cdots \\ a_N(f) \end{pmatrix}$$

2.2 Equivalent Electrical Circuit Model of an EAM

Besides modeling the characteristics of individual ECs, the design of complex PICs drives the necessity of modeling electronic-photonic interactions as well, in order to optimize the overall performance of the device. An optimized design of driving circuits of optical transmitter chips for example is very crucial for its performance in high speed operation.

As exemplary use case we present below the model of an electro-optical circuit comprising electrical driver and electro-absorption modulator (EAM). This circuit is a section enclosed in one of the designs of a monolithically-integrated InP transmitter developed in frame of the European research project MIRTHE [7]. The full device (fig. 4) is an I-Q transmitter consisting of a DFB laser followed by a 1:4 MMI splitter that distributes the signal to four arms. Each arm comprises an EAM and an optical phase shifter, with prefixed phases of 0°, 180°, 270° and 90°, needed for generating the required modulation. The EAM on each arm switches the phases on/off reflecting the modulation data applied through the electrical driving circuit. The four branches are joined via a 4:1 MMI coupler and its output is fed into an SOA for amplification purposes.

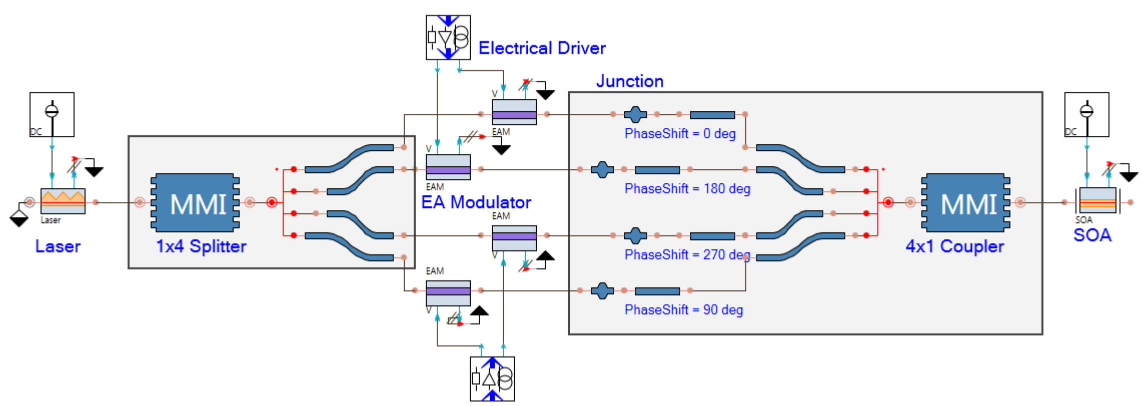

Fig. 4 Schematic of the simulated I-Q transmitter

The equivalent electrical circuit of EAMs was elaborated previously within the project GIBON [8]. It takes into account a dynamic junction voltage change induced by varying absorption and related photocurrent (represented by parallel dynamic resistance), RC crosstalk circuit between adjacent integrated sections and connecting wire inductance. The implementation of the equivalent EC of one of the arms with our new library models is represented in fig. 5. The parameters set in the elements correspond to EAM characteristics derived from measurements.

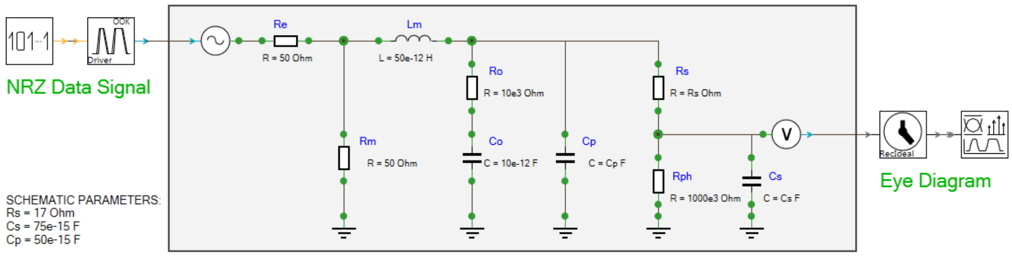

Fig. 5: Equivalent circuit of the EAM for 50Ohm impedance resistor and 50um length

Based on this design we vary individual values of electrical element parameters to investigate their impact on the overall EC performance. Exemplary, the calculated modulation response for two values of impedance resistor and different lengths of the EAM are represented in fig. 6.

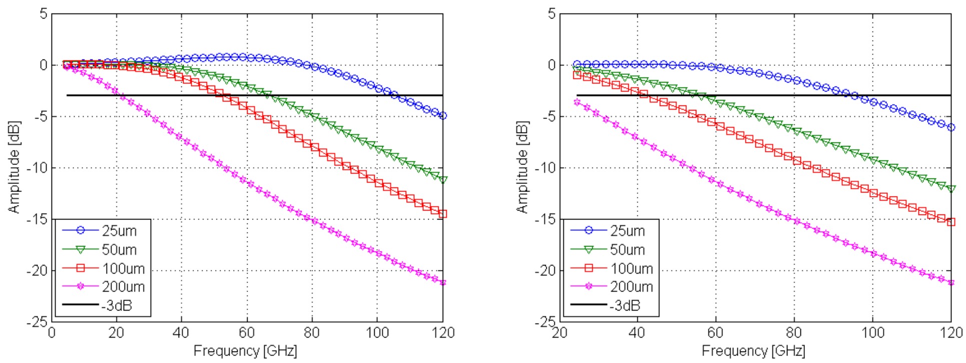

Fig. 6: Modulation response for different EAM lengths. Impedance matching 35Ohm (left) and 50Ohm (right)

For 50um long EAM, we found that the 3dB-bandwidth is approximately 65GHz for 35Ohm and 55GHz for 50Ohm impedances. The obtained characteristics are very similar to results obtained by measurements.

Further on, we tested the circuit with modulated NRZ signals at data rates of 50Gb/s and 100Gb/s. Results are represented in fig. 7. For the higher data rate, the eye diagram shows a much larger degree of distortion. Note that we have omitted (e.g. turned off) noise in the EC model in order to see clearly the signal shapes.

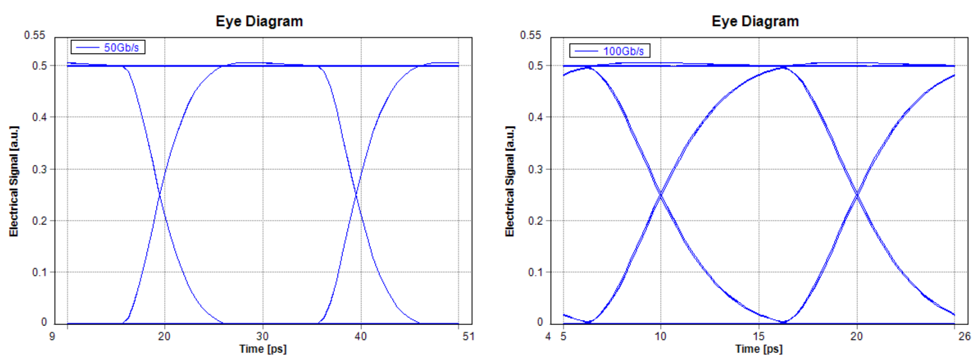

Fig. 7: Eye diagram at the output of the equivalent electrical circuit for 50Gb/s (left) and 100Gb/s (right)

More research on this field could be carried out by taking the equivalent EC model of a single EAM as basis, and extending it to represent the whole transmitter, including the drive signals as well. Design problems such as the effect of back reflections or the optimization of sub-element characteristics for increasing the modulation bandwidth can be investigated.

3. SCALABLE APPROACH FOR MODELING OPTO-ELECTRONIC CIRCUITS

With the example in the previous section we have demonstrated how to model and simulate an opto-electronic device by means of an equivalent electrical circuit and the S-matrix approach. Such solution works fine in the case of knowing the equivalent EC of photonic sub-elements, which is not always available or simply there is no equivalent electrical model capable of representing all optical effects. An integral circuit simulator should be able to combine photonic, electronic, active and passive elements on the same simulation setup. This is possible with our hybrid time-and-frequency-domain modeling (TFDM) approach for photonic integrated circuits, extended now to electrical circuits, explained next.

We take now a different example as illustration. It is based on an integrated recirculating optical buffer, as reported in [9]. To the original scheme, we have added three-ring add-drop filters for obtaining a different optical buffer capacity at different channel wavelengths (16-bit delay at 194.1 THz and 8-bit delay for all neighboring channels). The schematic of the device (fig. 8) consists of a 2x2 gate matrix switch formed by two MMI splitters and four SOAs. The gate matrix is connected to the delay line loops.

The input signal is split and directed to two of the SOAs (at the bottom). The split signals might be sent into the delay loop or to the output port, depending on the SOA states. The signal that enters into the loop is filtered out by the ring-filter. A different delay is applied to the original signal depending on its frequency. The delayed signal might be sent out the loop by switching on/off the corresponding SOAs. The switching control signal is applied to the SOA gates by means of an electrical driving circuit.

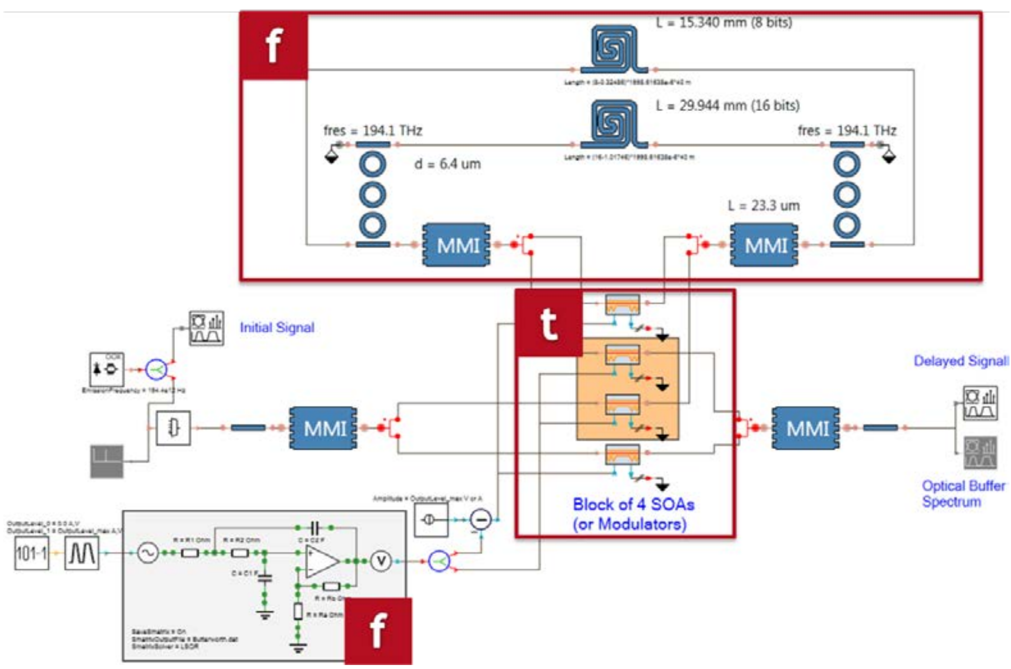

Fig. 8: Schematic of the recirculating optical buffer showing identified clusters of passive and active sub-elements

An adaptive electrical filter is used to control the driving signal for representing realistic bandwidth limitations in the electric circuit. The filter follows the Sallen-Key architecture of low-pass filters [10]. Such filters are known to support a rich variety of transfer functions, including the standard Butterworth, Chebyshev, and Bessel low-pass filters: the only difference between circuits that implement such filters are different values for the resistances R1 and R2, and capacitances C1 and C2 (see fig.1 for a close-up). The simulated circuit includes with an operational amplifier an active device as well, which is modeled in a linear approximation. Exemplary realizations of the filter for the different values of resistances and capacitances are represented in fig. 9.

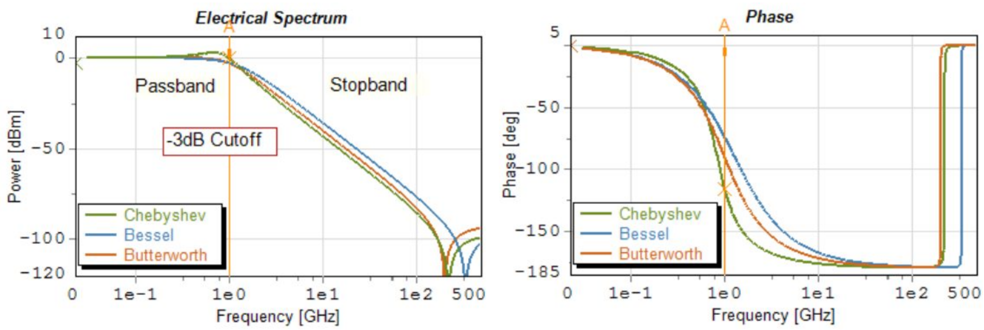

Fig. 9: Exemplary transfer characteristics of adaptive Sallen-Key low-pass filter

Continuing with our example, the inherent loss introduced at the input splitters and output combiners is compensated by the optical gain of the switch SOAs. A careful design of the amplifiers is required ensuring that low amplification noise as well as high extinction ratio and low crosstalk are provided. This is accomplished by accurate time-domain models that provide realistic results of non-linear effects such as saturation, spontaneous emission, chirp or internal reflections. Consequently, the passive optical filter and delay-line structures would need to be modeled in time-domain as well. Using the hybrid time-and-frequency domain modeling approach (as described in [2]), the whole topology is analyzed and clusters of connected passive photonic elements are identified. For each of these clusters, S-matrices of contained elements are recursively combined into a single S-matrix describing the cluster as a whole. This approach is also applied to the electrical sub-circuits being part of the overall electro-optical device. Designing FIR filters for these clusters can be accomplished with much higher accuracy compared to the individual passive sub-elements due to their larger dimensions. Fig. 8 shows the schematic of the recirculating optical buffer with identified clusters of passive sub-elements (marked with 'f').

Using the TFDM approach, high accuracy simulations of the given schematic are possible using small simulation bandwidths, and thus sample sizes. Fig. 10 depicts time-domain responses for the 194.1THz channel using sample rates of 640 GHz (right) and 2.56THz (left). In contrast, using the standard time-domain approach, one would need to employ sample rates exceeding 56 THz for accurate simulation results, which is impracticable. Moreover, the three-micro-ring optical filters in the schematic would set requirements to the quality of the designed digital filters that are extremely demanding and cannot be satisfied without using approximations of non-dispersive waveguides.

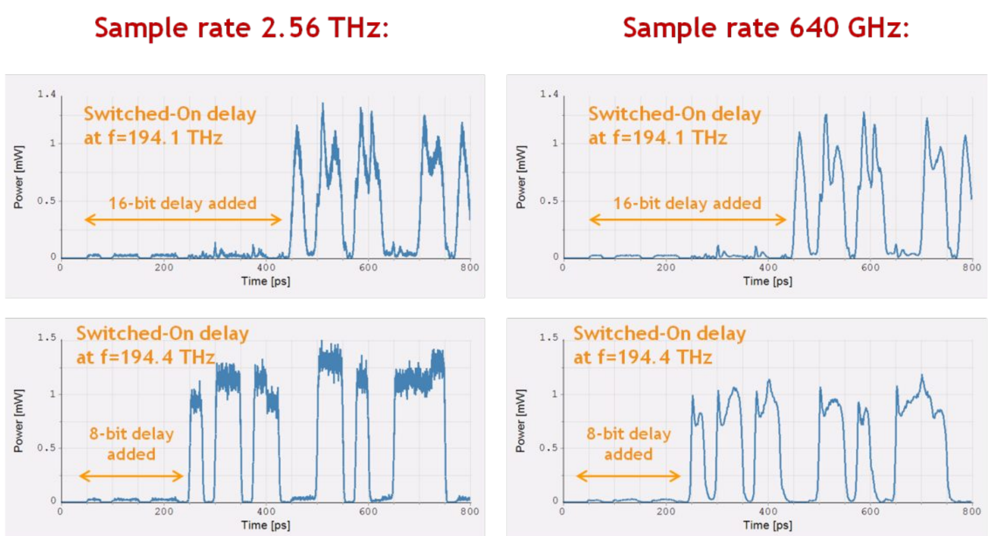

Fig. 10: Simulation results for the 194.1THz channel for two different simulation bandwidths

4. SUMMARY

With this work, we have presented a scalable approach for modeling opto-electronics integrated circuits in the context of the professional design suite *VPIcomponentMaker Photonic Circuits*. We have shown the enhanced capabilities for modeling electric and photonic circuits integrated in the same simulation setup. This is accomplished by the extension of the S-matrix simulation domain to electrical elements and applying our earlier presented hybrid time-and-frequency-domain modeling (TFDM) approach. We showed application examples highlighting the importance to combine different circuit-level modeling techniques within the same simulation setup in order to model realistic opto-electronic devices efficiently.

REFERENCES

[1] Arellano, C., Mingaleev, S.F., Sokolov, E., Koltchanov I., Richter A., "Efficient Design of Photonic Integrated Circuits (PICs)," ICTON, paper Th.A4.1 (2011).

[2] Arellano, C., Mingaleev, S.F., Sokolov, E., Koltchanov I., Richter A., "Time-and-Frequency-Domain Modeling (TFDM) of Hybrid Photonic Integrated Circuits," OPTO Photonics West, paper 8265-19 (2012).

[3] Ho, C. W., Ruehli, A. and Brennan, P., "The modified nodal approach to network analysis," IEEE Transactions on Circuits and Systems, Vol. 22, No. 6, 504-509 (1975).

[4] Vladimirescu, A., [The SPICE book], John Wiley & Sons, (1994).

[5] Smy, T., and Gunupudi, P. "Addressing practical issues with banded-variables in an MNA-based optoelectronic simulation framework," 14th Workshop on Signal Propagation on Interconnects (2010).

[6] Montgomery, C., Dicke, R. H. and Purcell, E. M., [Principles of Microwave Circuits], M. I. T. Rad. Lab. Ser., vol. 8 McGraw-Hill Book Co., (1948).

[7] http://www.ist-mirthe.eu/

[8] http://www.ist-gibon.eu/

[9] Park, H., Mack, J.P., Blumenthal, D.J., and Bowers, J.E., "An integrated recirculating optical buffer," Opt. Express 16, 11124 (2008).

[10] "Analysis of the Sallen-Key Architecture," Application Report by Texas Instruments (2002).